Supplementary information for the manuscript:

Sulindac Sulfide Induces the Formation of Large Oligomeric Aggregates of the Alzheimer's Disease Amyloid-β Peptide Which Exhibit Reduced Neurotoxicity

Authors:

Elke Prade[1], Dr. Christian Barucker[2], Dr. Riddhiman Sarkar[1], Dr. Gerhard Althoff-Ospelt[3], Dr. Juan Miguel Lopez del Amo[4], Shireen Hossain[2], Yifei Zhong[2], Prof. Dr. Gerd Multhaup[2], Prof. Dr. Bernd Reif*[1,5]

Affiliations:

[1] Munich Center for Integrated Protein Science (CIPS-M) at Department Chemie, Technische Universität München (TUM), Lichtenbergstr. 4, 85747 Garching, Germany.

[2] Department of Pharmacology & Therapeutics, McGill University, 3655 Promenade Sir-William-Osler, Montreal QC, H3G 1Y6, Canada.

[3] Bruker BioSpin, Silberstreifen 4, 76287 Rheinstetten, Germany.

[4] Current address: CIC Energigune, Albert Einstein 48, 01510 Miñano, (Álava), Spain.

[5] Helmholtz-Zentrum München (HMGU), Deutsches Forschungszentrum für Gesundheit und Umwelt, Ingolstädter Landtstr. 1, 85764 Neuherberg, Germany.

* Email: reif@tum.de

Table of Contents

Results

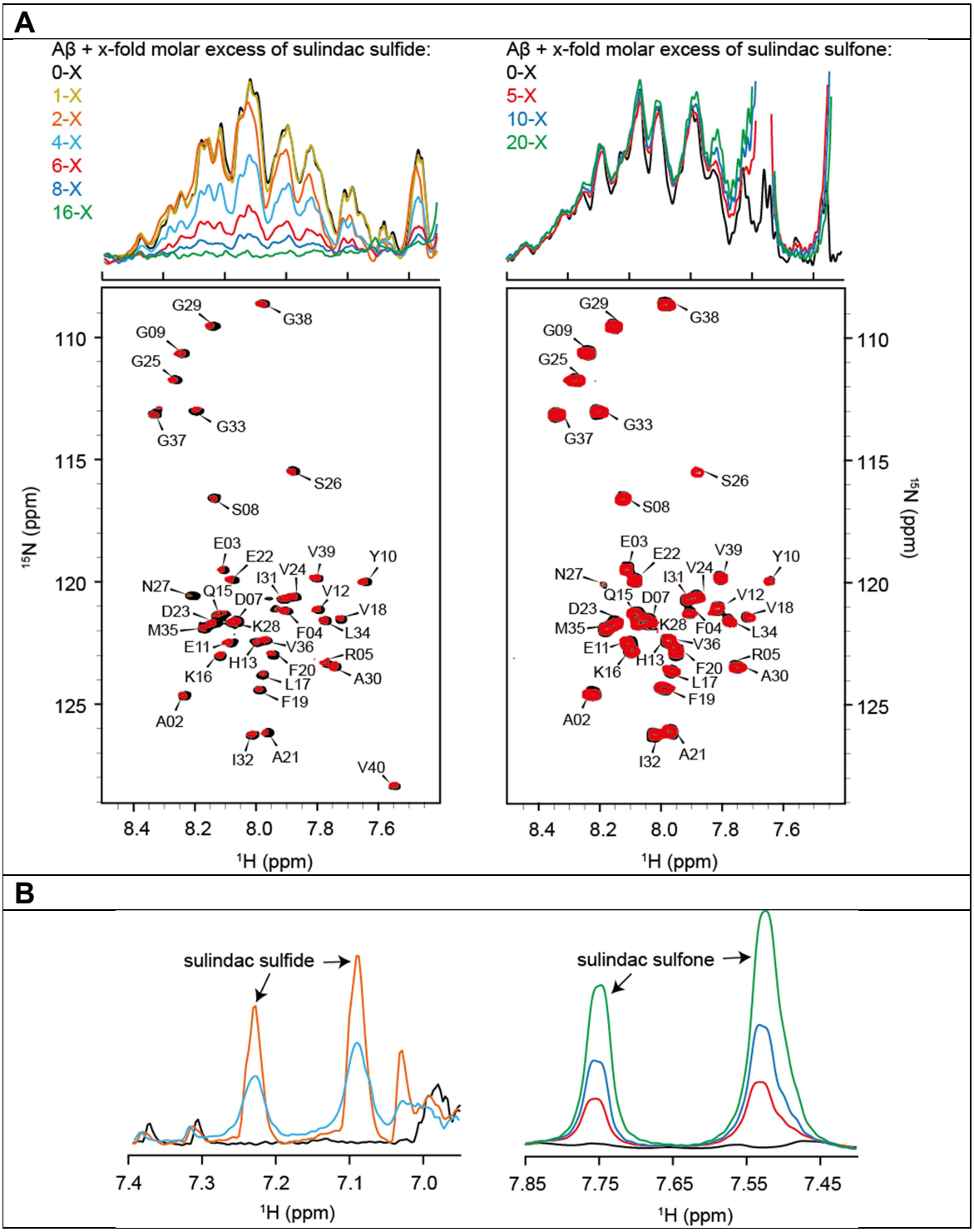

Supplementary Figure 1: Solution-state NMR of Aβ and NSAIDs. (A) ^{1}H-1D NMR spectra of monomeric Aβ in the presence of increasing concentrations of sulindac sulfide (left) and sulindac sulfone (right), as well as ^{1}H-^{15}N HSQC of Aβ in the absence (black) and presence (red) of a 6-fold molar excess of sulindac sulfide (left) and

sulindac sulfone (right). Loss of signal intensities are observed with increasing concentrations of the NSAID, indicating aggregation of Aβ. (B) ^{1}H-1D NMR spectra of characteristic signals of sulindac sulfide (left) and sulindac sulfone (right) in the presence of a 50 µM monomeric Aβ solution. Signal intensities are attenuated and broadened at a 4-fold molar excess of sulindac sulfide (blue) compared to lower concentrations (orange), whereas NMR signals of sulindac sulfone show an increase in peak intensity corresponding to the increase in NSAID concentration.

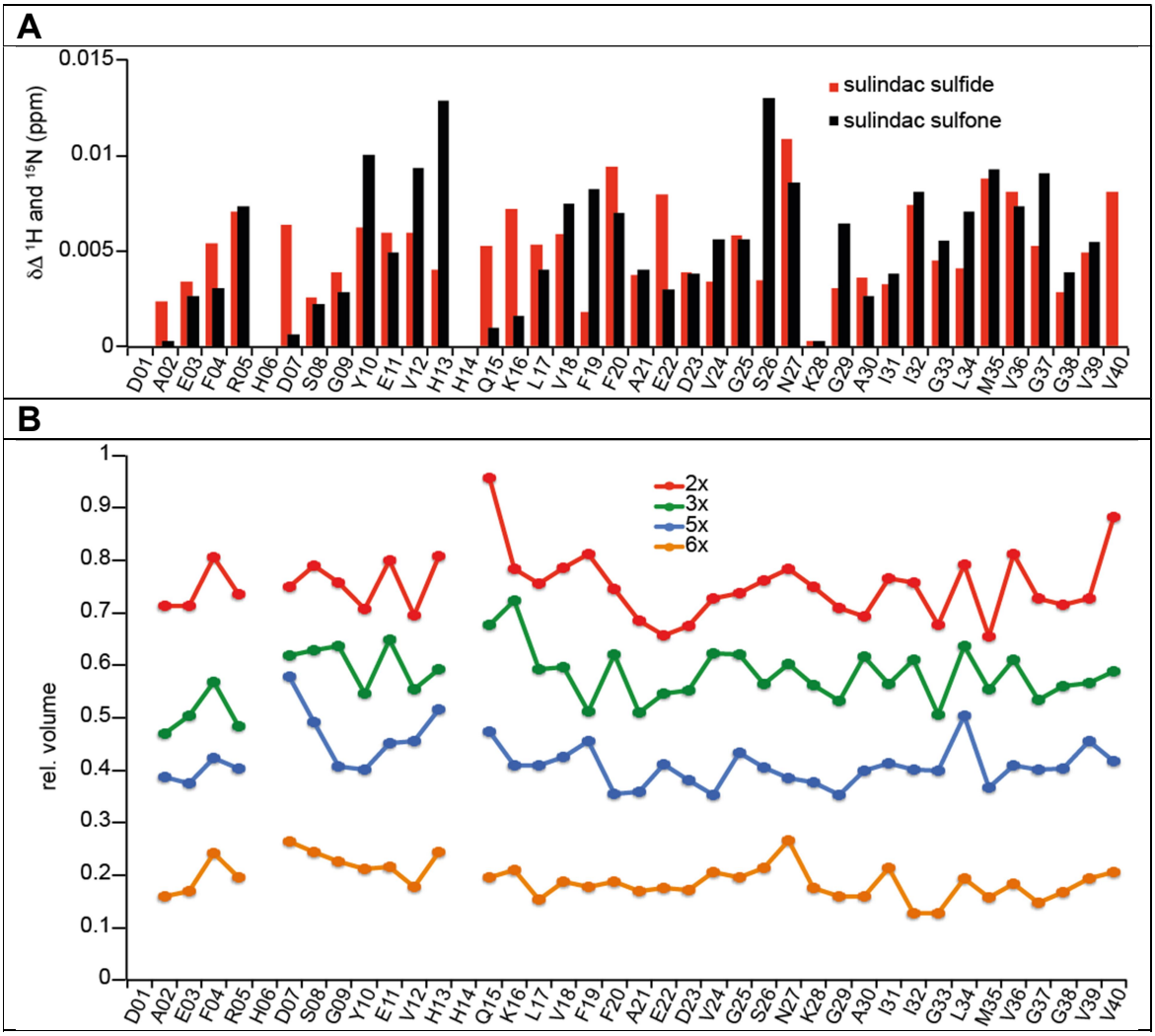

Supplementary Figure 2: Analysis of solution-state NMR of Aβ and NSAIDs. (A) CSPs Δδ (ppm) observed for Aβ in the presence of 5-fold molar excesses of sulindac sulindac sulfide (red) and sulindac sulfone (black) compared to monomeric Aβ. (B) Relative volumes of Aβ incubated in the presence of increasing amounts of sulindac sulfide extracted from ^{1}H-^{15}N HSQC signals.

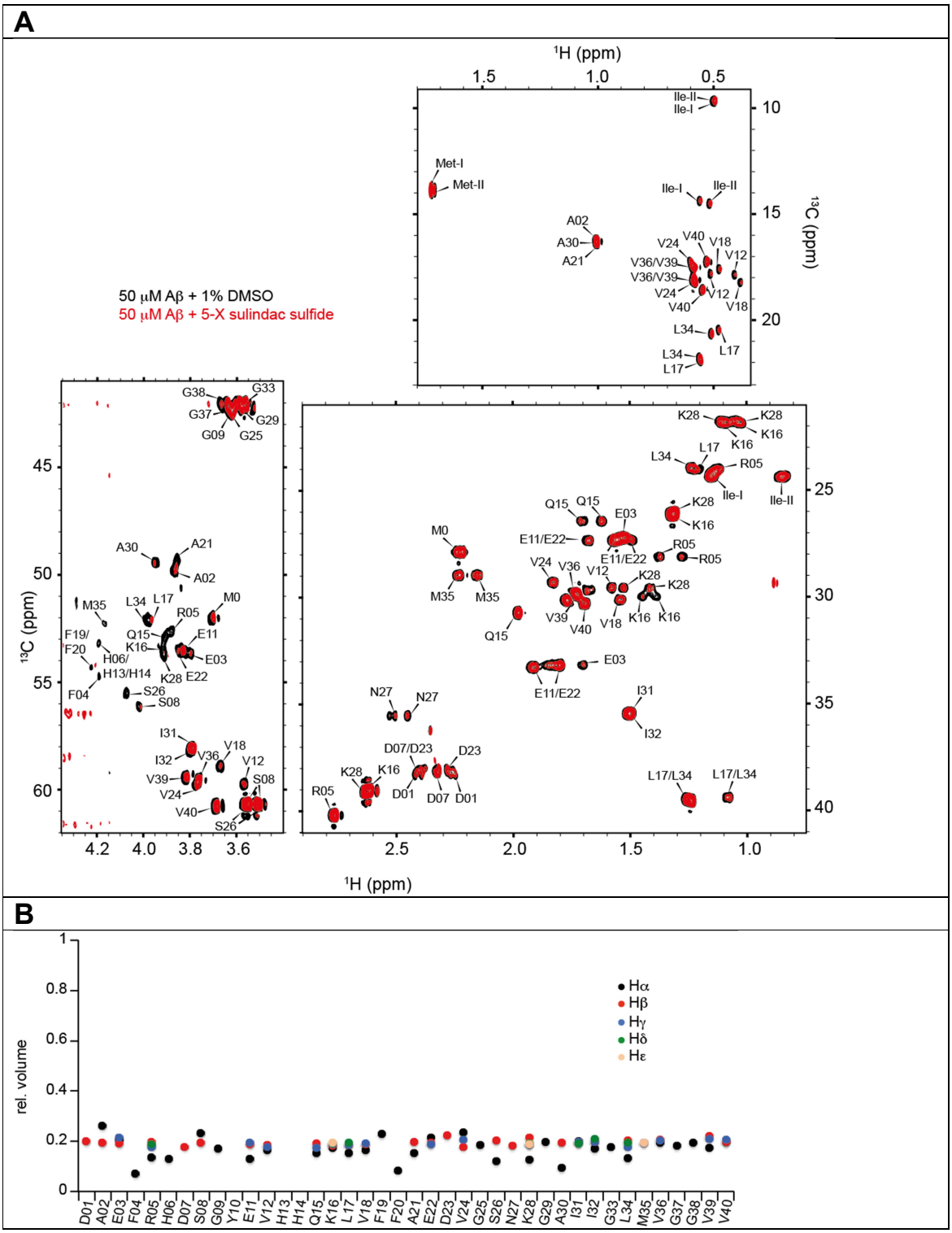

Supplementary Figure 3: Solution-state NMR studies of Aβ sidechains and NSAIDs. (A) ^{1}H-^{13}C HSQC of Aβ in the presence of a 5-fold molar excess of sulindac sulfide (red) and 1% DMSO as a control (black). (B) relative volumes of ^{1}H-^{13}C Aβ cross-peaks in the presence of a 5-fold molar excess of sulindac sulfide.

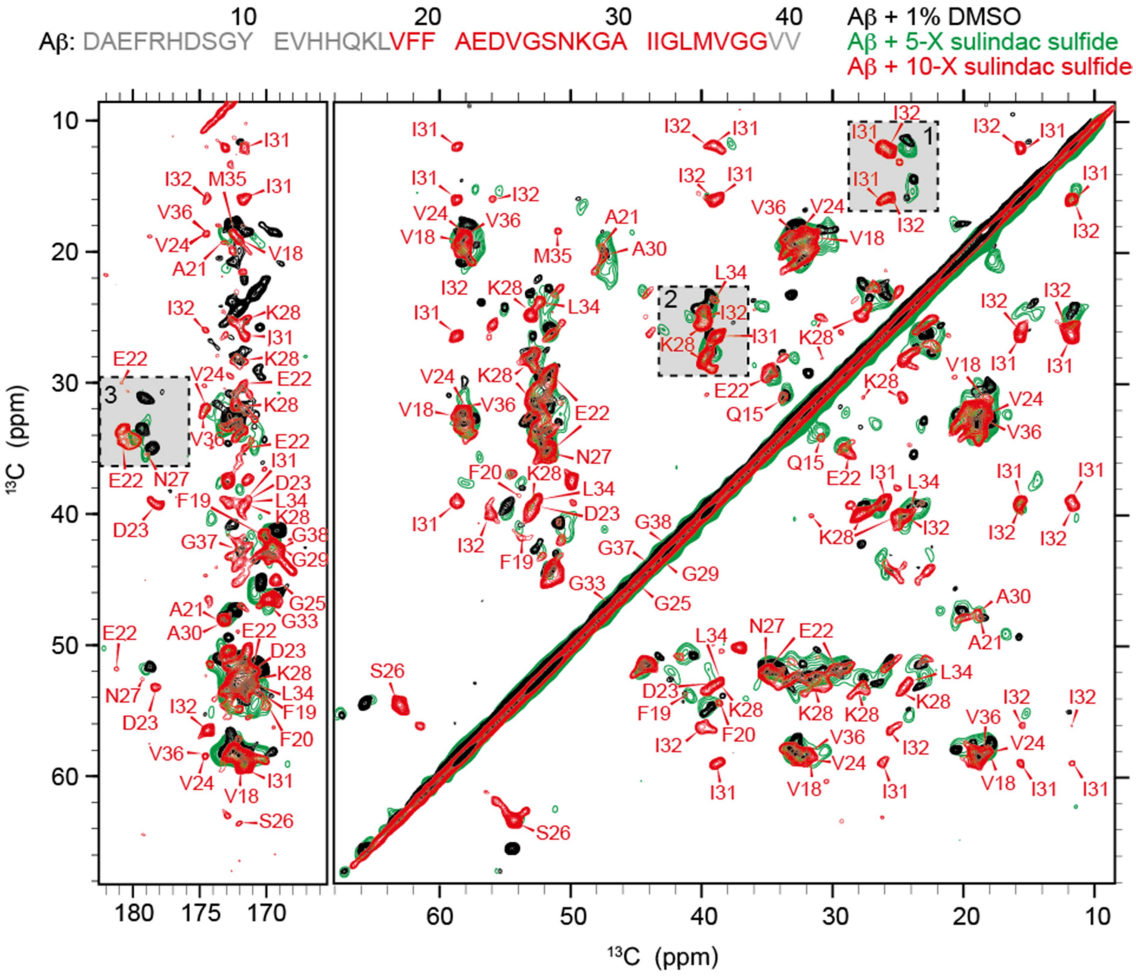

Supplementary Figure 4: Solid-state NMR spectra of NSAID induced Aβ aggregates. ^{13}C-^{13}C PDSD correlation spectrum of Aβ aggregated in the presence of a 5-fold (green) and 10-fold (red) molar excess of sulindac sulfide and 1% DMSO after 1 day, as well as Aβ in the presence of only 1% DMSO (black) as a control. NCACX and NCOCX experiments allowed sequential assignment of chemical shifts of individual resonances for residues E22-G38 for Aβ incubated in the presence of a 10-fold molar excess of sulindac sulfide (red). Squares indicated 1-3 are magnified in Fig. 3A.

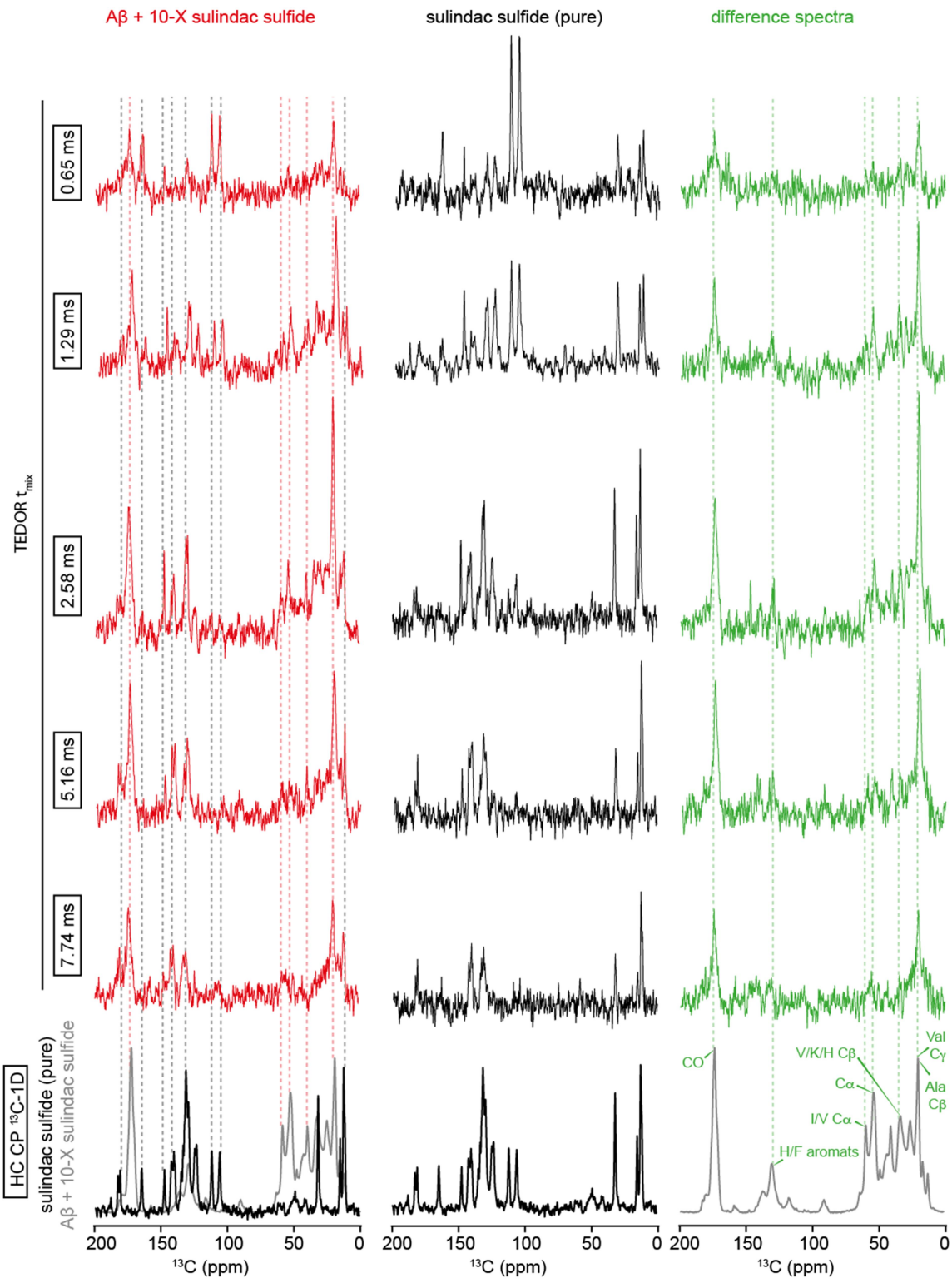

Supplementary Figure 5: ^{13}C-^{19}F TEDOR spectra of NSAID induced Aβ aggregates. ^{13}C-^{19}F TEDOR spectra to detect dipolar contacts between ^{13}C and ^{19}F atoms in Aβ aggregates induced by sulindac sulfide (red), and for pure sulindac sulfide (black), respectively. The experiments were run with mixing times of 0.65, 1.29, 2.58, 5.16 and 7.74 ms. The sulindac sulfide spectra were subtracted from the spectrum obtained for Aβ aggregates with a

factor 0.5 to yield the difference spectra (green). In the lowest row, the HC CP ^{13}C-1D experiments which show all ^{13}C atoms in Aβ aggregates (gray) and pure sulindac sulfide (black) is represented. Vertical connecting lines are drawn to the full ^{13}C spectra to guide the eye.

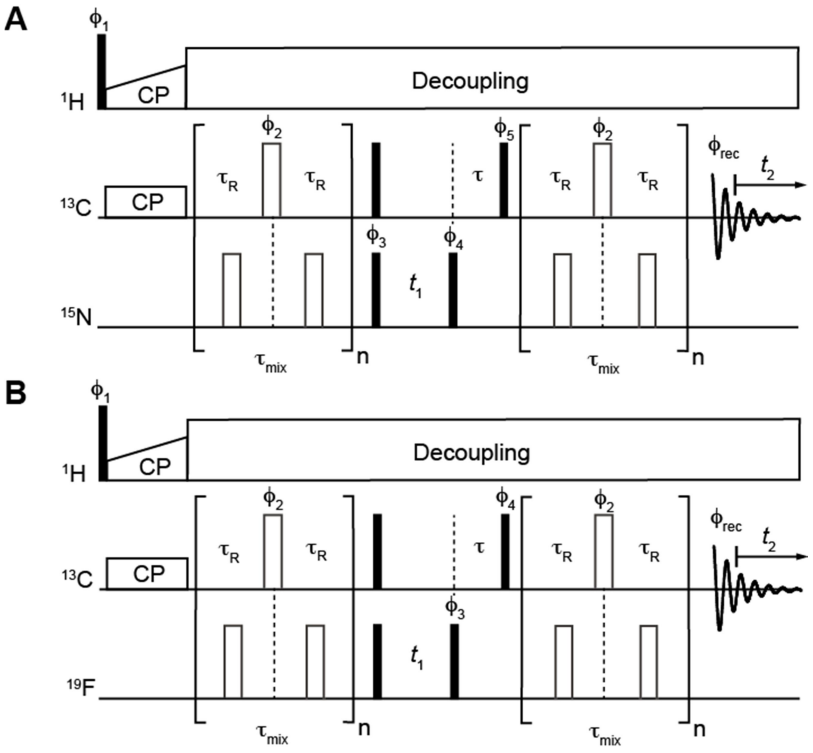

Supplementary Figure 6: Solid-state NMR pulse sequences. (A) ^{13}C-^{15}N TEDOR pulse sequence used to detect the D23Cγ - K28Nζ salt bridge and (B) ^{13}C-^{19}F TEDOR pulse sequence used to detect ^{13}C atoms near the ^{19}F- atom of sulindac sulfide. The pulse sequences are based on the 3D TEDOR experiments described by Jaroniec *et al.*[1] Black rectangles represent π/2-pulses and white rectangles represent π-pulses. Both experiment start with a ^{1}H-^{13}C CP transfer. The TEDOR sequences consists of two REDOR periods, which allow to transfer magnetization from ^{13}C to S spins, followed by an evolution period t_1. The experiment to detect the salt bridge was recorded in 2D-mode; the experiment to identify ^{19}F nuclei near ^{13}C atoms was recorded in 1D-mode. The following phase-cycles were used: (A) ϕ_1 = y, -y; ϕ_2 = y; ϕ_3 = x, x, -x, -x; ϕ_4 = -x; ϕ_5 = y, y, y, y, -y, -y, -y, -y; ϕ_{rec} = x, -x, -x, x, -x, x, x, -x; the REDOR π-pulses on ^{15}N are phase-cycled employing the xy-16 scheme.[2] (B) ϕ_1 = y, -y; ϕ_2 = y; ϕ_3 = x, x, -x -x; ϕ_4 = (x)*4, (y)*4, (-x)*4 (-y)*4; ϕ_{rec} = -x, x, x, -x, y, -y, -y, y, x, -x, -x, x, -y, y, y, -y. The REDOR π-pulses on the ^{19}F-spins are phase-cycled eomplyoing the xy-16 scheme. The phases for all other pulses were set to x.

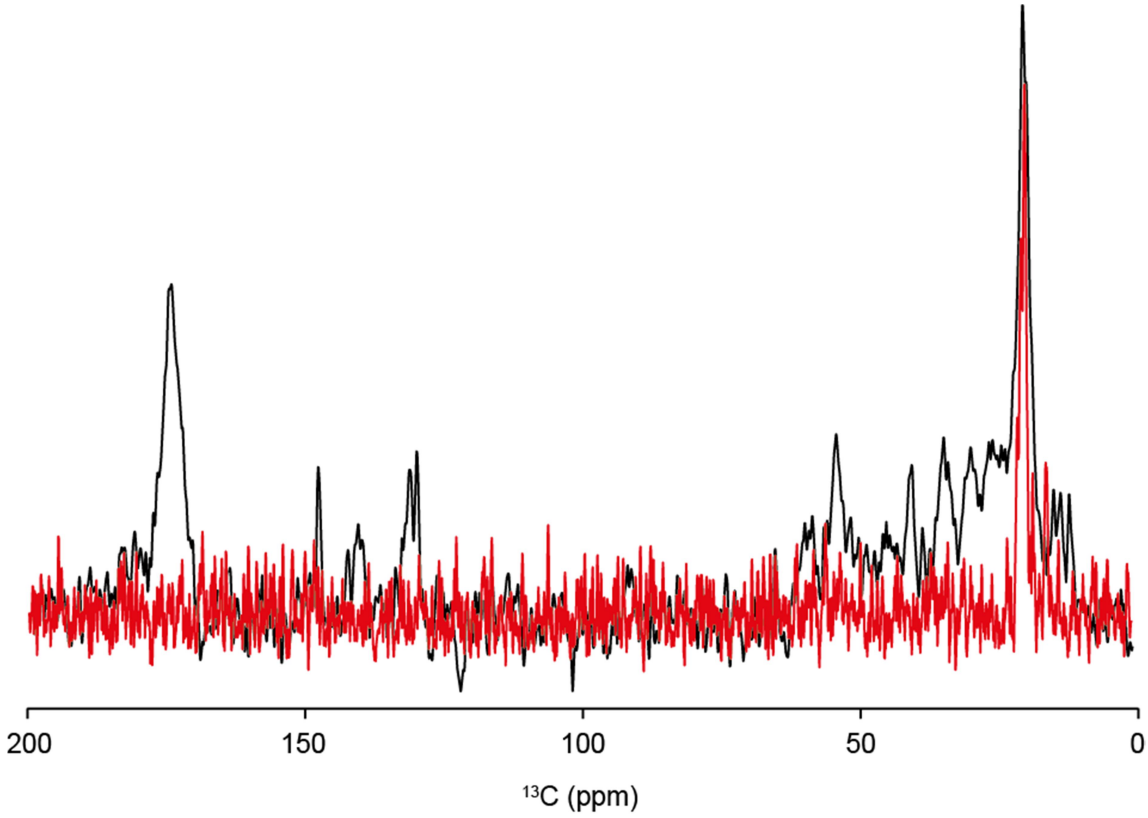

Supplementary Figure 7: Comparison of ^{13}C-^{19}F dipolar contacts between sulindac sulfide and Aβ fibrils or induced Aβ aggregates. Black: ^{13}C-^{19}F TEDOR spectrum for a sample in which sulindac sulfide was titrated to monomeric Aβ using a 10-fold molar excess of sulindac sulfide. The TEDOR mixing time was set to of 2.58 ms. Red: ^{13}C-^{19}F REDOR spectrum for a sample in which a 5-fold molar excess of sulindac sulfide was titrated to preformed Aβ fibrils.[3] In this experiment, the mixing time was set to 4.4 ms.

aa	N	CO	Cα	Cβ	Cγ	Cδ	Cε	Nζ
V18	-	171.83	58.27	32.25	18.73	-	-	
F19	131.00	170.35	53.33	41.27		128.84		
F20	128.77	169.74	54.15	38.62		129.96	128.25	
A21	127.50	173.07	47.75	19.12	-	-	-	
E22	126.69	171.44	51.49	29.63	34.51	181.30	-	
D23	121.89	171.38	52.84	39.06	178.56	-	-	
V24	120.97	174.46	57.97	31.62	18.29	-	-	
G25	115.63	169.25	44.75	-	-	-	-	
S26	108.56	171.97	54.47	63.10	-	-	-	
N27	125.26	170.33	52.03	35.14	179.51	-	-	
K28	131.22	171.59	52.85	31.18	24.94	27.84	39.32	36.8
G29	115.15	169.36	42.21	-	-	-	-	
A30	130.05	173.15	47.60	19.82	-	-		
I31	127.18	171.42	58.40	38.77	15.43 26.08	11.76		-
I32	129.06	174.46	55.99	39.61	15.52 25.34	11.74		-
G33	121.73	169.49	45.97	-	-	-		
L34	120.88	171.84	50.72	43.91	25.15	23.05 22.46		-
M35	122.16	172.32	50.79	-	31.26	-	18.47	
V36	-	174.88	57.66	32.13	18.16	-	-	
G37	111.25	171.63	42.28	-	-	-	-	
G38	112.67	169.52	41.94	-	-	-	-	

Supplementary Table 1: Chemical shifts assigned for Aβ aggregates induced by a 10-fold molar excess of sulindac sulfide.

References

[1] Jaroniec, C. P., Filip, C., and Griffin, R. G. (2002) 3D TEDOR NMR experiments for the simultaneous measurement of multiple carbon-nitrogen distances in uniformly (13)C,(15)N-labeled solids, *J. Am. Chem. Soc. 124*, 10728-10742.

[2] Gullion, T., Baker, D. B., and Conradi, M. S. (1990) New, compensated Carr-Purcell sequences, *J. Magn. Reson. 89*, 479-484.

[3] Prade, E., Bittner, H. J., Sarkar, R., Lopez Del Amo, J. M., Althoff-Ospelt, G., Multhaup, G., Hildebrand, P. W., and Reif, B. (2015) Structural Mechanism of the Interaction of Alzheimer Disease Abeta Fibrils with the Non-steroidal Anti-inflammatory Drug (NSAID) Sulindac Sulfide, *J. Biol. Chem. 290*, 28737-28745.